

DIRECT REACTIONS WITH EXOTIC BEAMS 2022



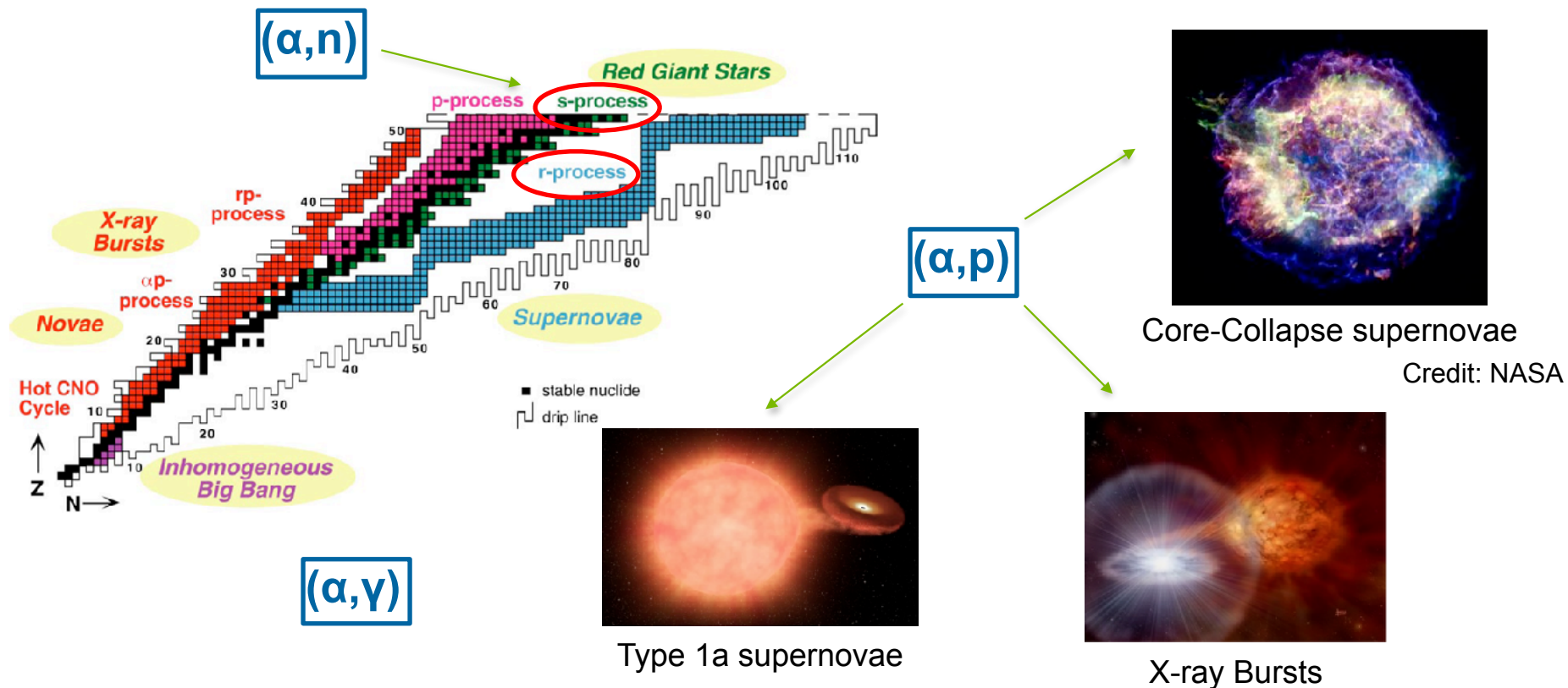
Direct measurement of the $^{22}\text{Mg}(\alpha, p)^{25}\text{Al}$ reaction using MUSIC relevant for Type I X-ray bursts



Heshani Jayatissa
Argonne National Laboratory

June 28, 2022
Santiago de Compostela, ES

Alpha-induced reactions for nuclear astrophysics



Importance of (α ,p) reactions for X-ray bursts

Before the XRB:

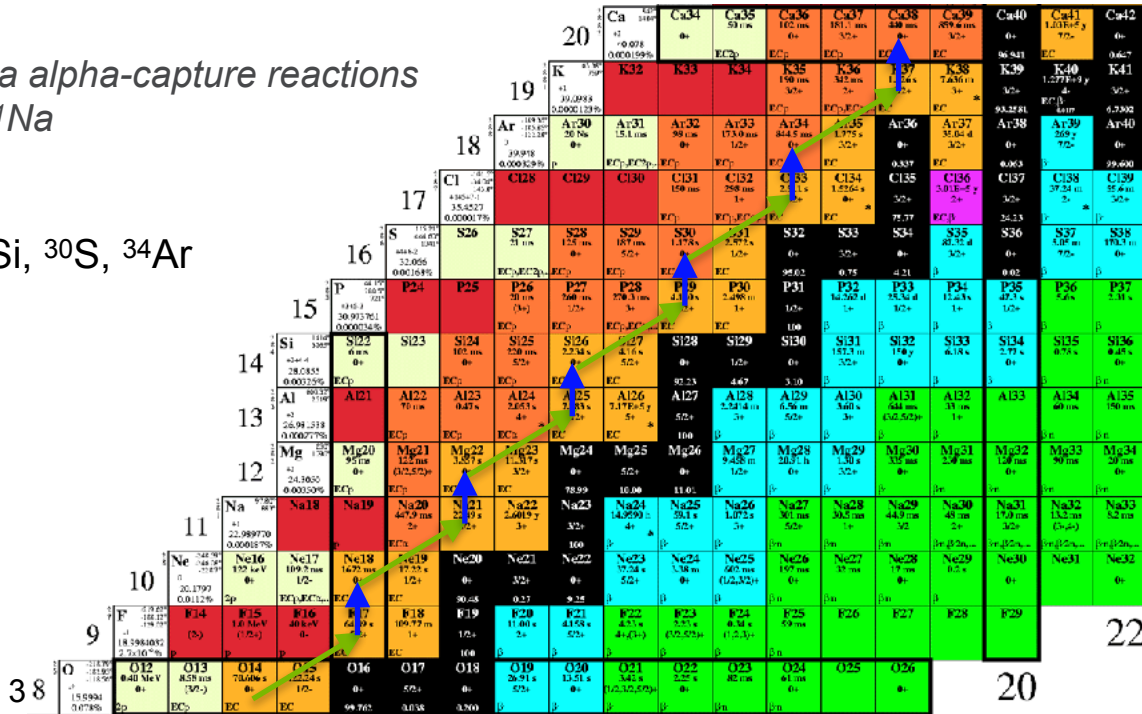
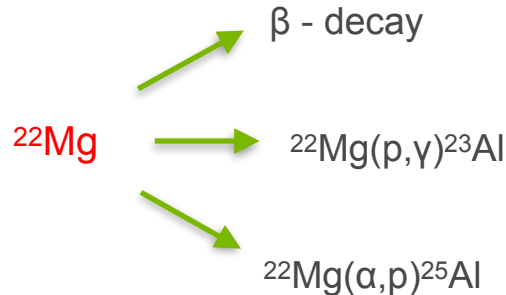
H is burnt via the hot CNO cycle \longrightarrow powered by 3α reaction \longrightarrow thermonuclear runaway

During the XRB:

Breaks out of the hot CNO cycle via alpha-capture reactions

$^{15}\text{O}(\alpha,\gamma)^{19}\text{Ne}$ & $^{18}\text{Ne}(\alpha,p)^{21}\text{Na}$

A few waiting point nuclei : ^{22}Mg , ^{26}Si , ^{30}S , ^{34}Ar



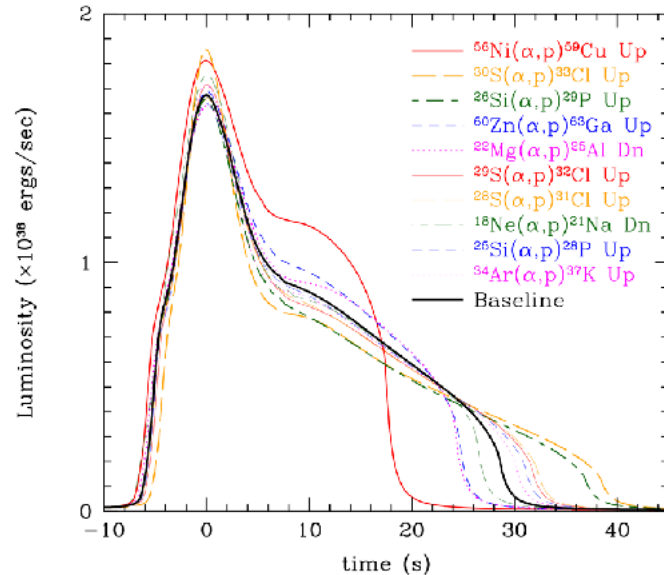
Importance of XRB models



- Comparisons between XRB models and observed light curves allows to constrain elements of neutron stars:
 - Composition
 - Mass-Radius ratio
 - Compactness
 - Accretion rate
 - Accretion-based heating
- Models also allow predictions of the XRB ashes which alters the composition of the neutron star crust.
- XRB models are sensitive to nuclear physics inputs such as reaction rates.

XRB SENSITIVITY STUDY

Cyburt et al. (2016)



R. H. Cyburt et al. (2016)

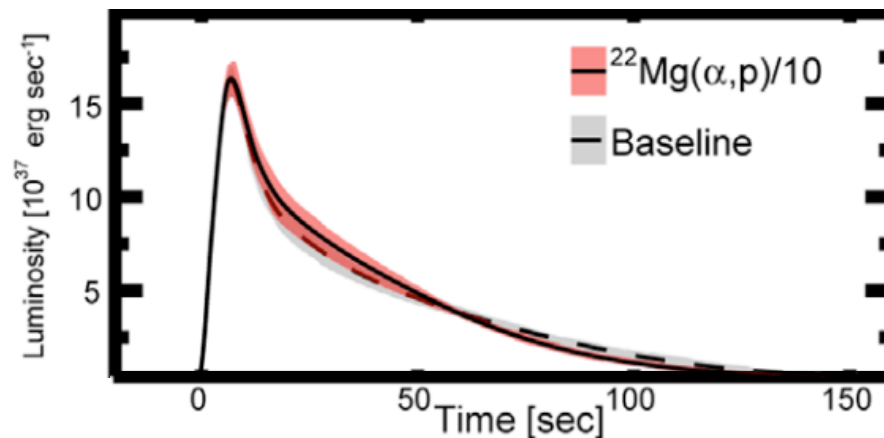
Rank	Reaction	Type ^a	Sensitivity ^b	Category
1	$^{15}\text{O}(\alpha, \gamma)^{19}\text{Ne}$	D	16	1
2	$^{56}\text{Ni}(\alpha, p)^{59}\text{Cu}$	U	6.4	1
3	$^{59}\text{Cu}(p, \gamma)^{60}\text{Zn}$	D	5.1	1
4	$^{61}\text{Ga}(p, \gamma)^{62}\text{Ge}$	D	3.7	1
★ 5	$^{22}\text{Mg}(\alpha, p)^{25}\text{Al}$	D	2.3	1
6	$^{14}\text{O}(\alpha, p)^{17}\text{F}$	D	5.8	1
7	$^{23}\text{Al}(p, \gamma)^{24}\text{Si}$	D	4.6	1
8	$^{18}\text{Ne}(\alpha, p)^{21}\text{Na}$	U	1.8	1
9	$^{63}\text{Ga}(p, \gamma)^{64}\text{Ge}$	D	1.4	2
10	$^{19}\text{F}(p, \alpha)^{16}\text{O}$	U	1.3	2
11	$^{12}\text{C}(\alpha, \gamma)^{16}\text{O}$	U	2.1	2
12	$^{26}\text{Si}(\alpha, p)^{29}\text{P}$	U	1.8	2
13	$^{17}\text{F}(\alpha, p)^{20}\text{Ne}$	U	3.5	2
14	$^{24}\text{Mg}(\alpha, \gamma)^{28}\text{Si}$	U	1.2	2
15	$^{57}\text{Cu}(p, \gamma)^{58}\text{Zn}$	D	1.3	2
16	$^{60}\text{Zn}(\alpha, p)^{63}\text{Ga}$	U	1.1	2
17	$^{17}\text{F}(p, \gamma)^{18}\text{Ne}$	U	1.7	2
18	$^{40}\text{Sc}(p, \gamma)^{41}\text{Ti}$	D	1.1	2
19	$^{48}\text{Cr}(p, \gamma)^{49}\text{Mn}$	D	1.2	2

SENSITIVITY STUDY

Meisel et al. (2019)

Studied the impact of the 19 reactions identified by Cyburt et al. in model-observation comparisons for XRBs

☆ $^{15}\text{O}(\alpha,\gamma)$	$^{22}\text{Mg}(\alpha,p)$
☆ $^{23}\text{Al}(p,\gamma)$	$^{24}\text{Mg}(\alpha,\gamma)$
$^{14}\text{O}(\alpha,p)$	$^{59}\text{Cu}(p,\gamma)$
$^{18}\text{Ne}(\alpha,p)$	$^{61}\text{Ga}(p,\gamma)$



Reaction rate of $^{22}\text{Mg}(\alpha,p)$ from theoretical Hauser-Feshbach was divided by a factor of 10 to assess the light curve impact.

This effects the XRB light curve tail due to the enhancement of hydrogen burning early in the burst via $^{22}\text{Mg}(p,\gamma)^{23}\text{Al}(p,\gamma)^{24}\text{Si}$

Indirect measurement using $^{28}\text{Si}(p,t)^{26}\text{Si}$

A. Matic et al. (2011)

TABLE III. The adopted S_α and spin values and resonance strengths for the four resonances in the $^{22}\text{Mg}(\alpha,p)^{25}\text{Al}$ reaction.

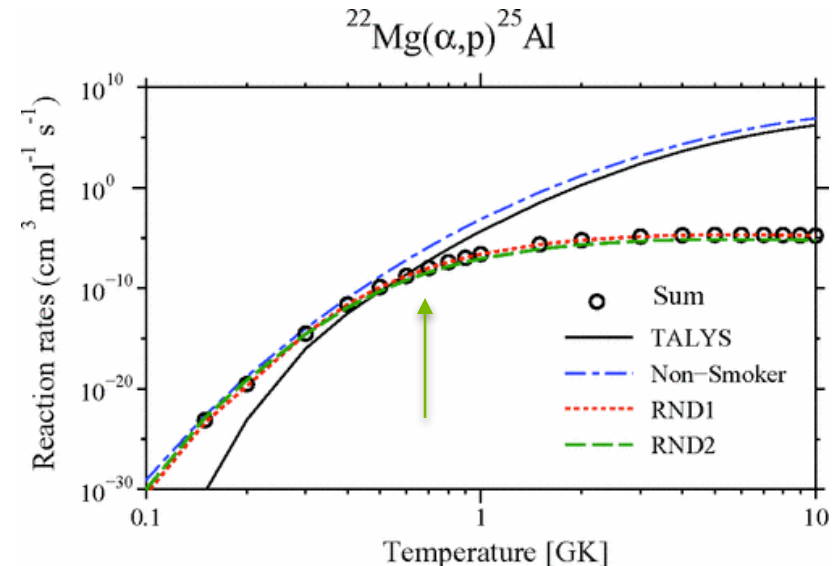
E_x (^{26}Si) (MeV)	E_{res} (MeV)	J^π	S_α	J	Mirror ^a $\omega\gamma$ (eV)	J	RND1 ^b $\omega\gamma$ (eV)	J	RND2 ^b $\omega\gamma$ (eV)
9.316	0.152	$[4^+]$	0.015	4	5.81×10^{-37}	1	6.22×10^{-35}	4	5.81×10^{-37}
9.605	0.441	$[2^+]$	0.037	2	1.20×10^{-14}	1	6.66×10^{-15}	0	1.98×10^{-14}
9.762	0.598	$[5^-]$	0.007	5	3.72×10^{-13}	5	3.72×10^{-13}	2	1.23×10^{-10}
9.903	0.739	$[0^+]$	0.037	0	5.14×10^{-08}	0	5.14×10^{-08}	1	1.79×10^{-08}

^aSpin and resonance strength for the mirror assignments.

^bSpin and resonance strength for the randomly generated spins of states.

- Observed 4 resonances in ^{26}Si above alpha threshold.
- Uncertainty in spin-parities of the measured states and the lack of resonance data above $E_x = 10$ MeV
- Reaction rate for $^{22}\text{Mg}(\alpha,p)$ is significantly lower than predicted by HF calculations for $T > 0.7$ GK.

PRC 84, 025801 (2011)

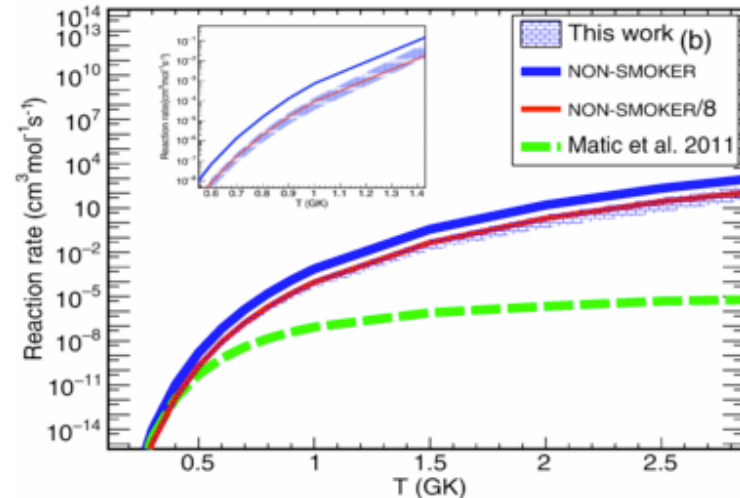
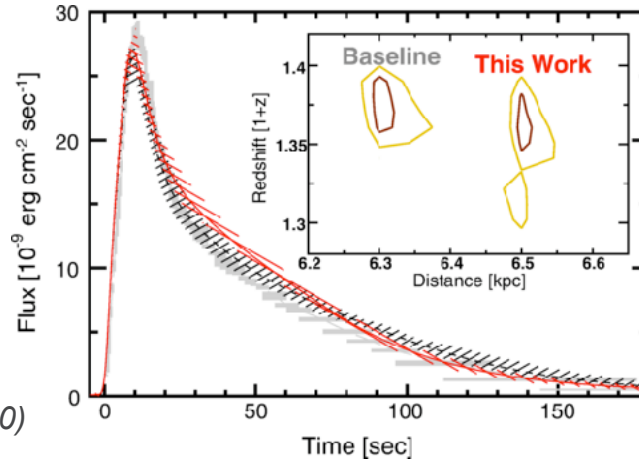
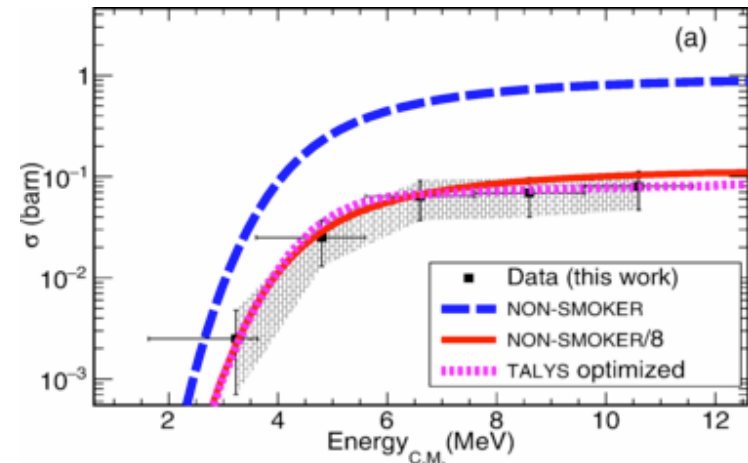


First direct measurement

J. S. Randhawa et al. (2020)

^{22}Mg 5 MeV/u on He:CO₂ gas target in AT-TPC

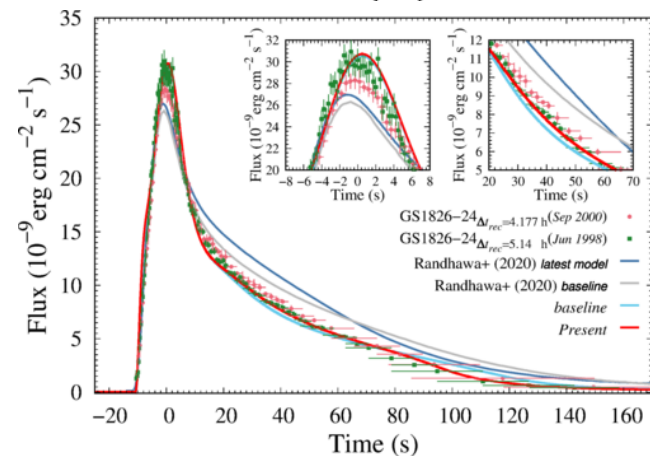
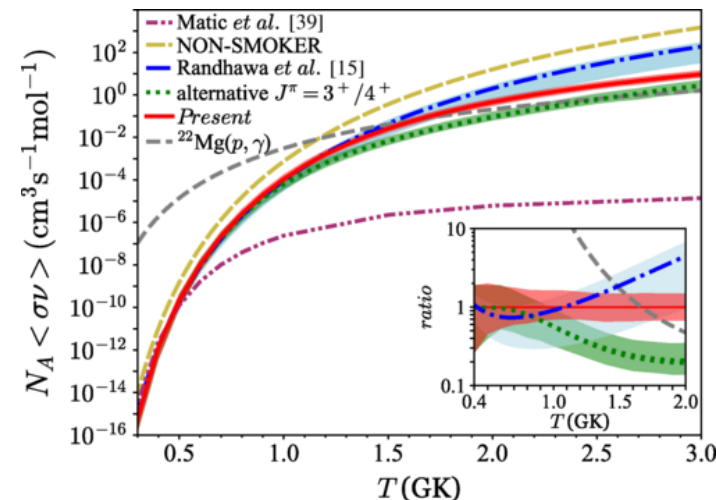
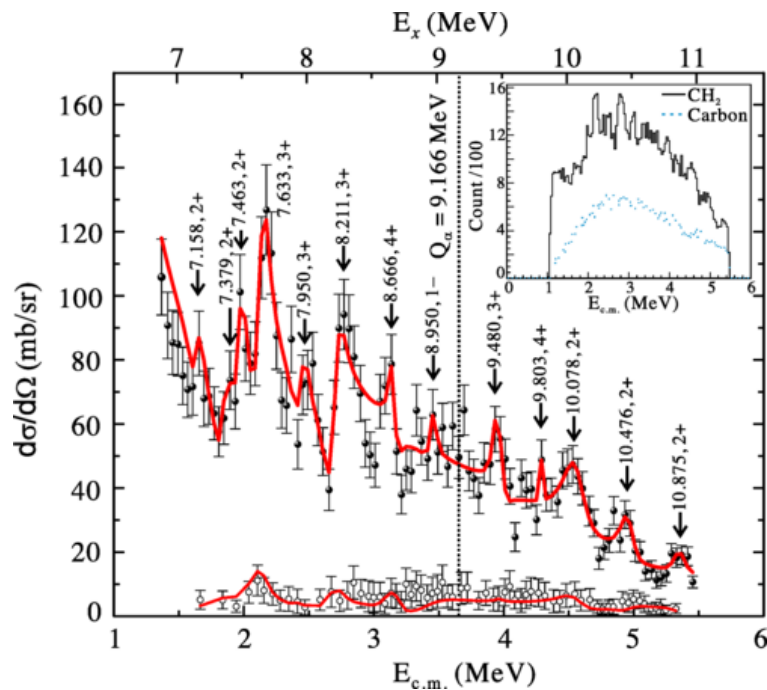
Reaction CS is in agreement with theoretical Hauser-Feshbach cross sections using NON-SMOKER divided by a **factor of 8** !!



PRL 125, 202701 (2020)

(In)elastic scattering using $^{25}\text{Al} + \text{p}$

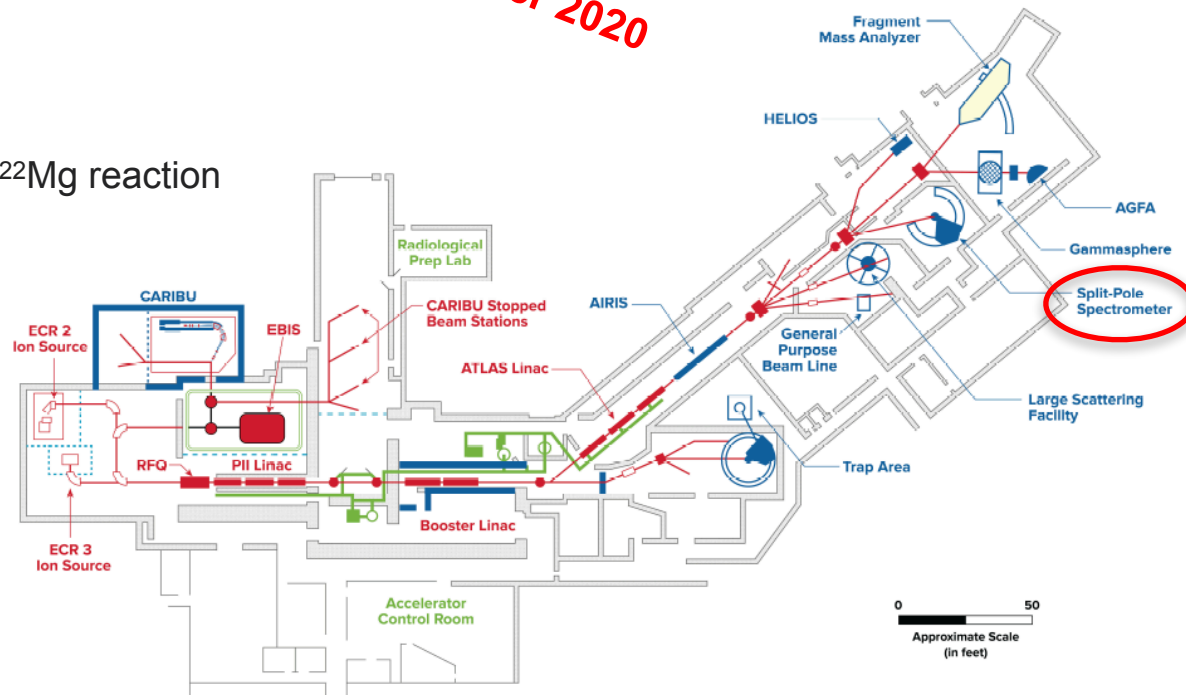
J. Hu et al. (2021)



Experiment details

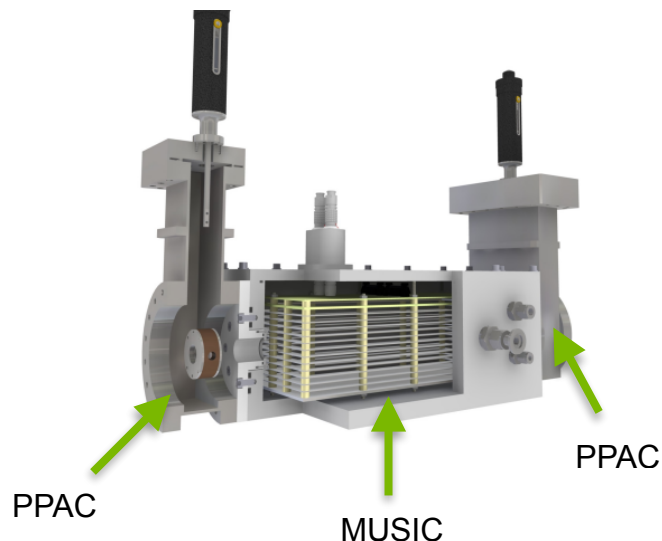
- Primary beam - ^{20}Ne
- ^{22}Mg created through $^{20}\text{Ne}(^3\text{He},n)^{22}\text{Mg}$ reaction
- 74 MeV secondary ^{22}Mg beam
- Beam intensity $\sim 150\text{-}200$ pps
- Pure He gas target at 400 torr

December 2020

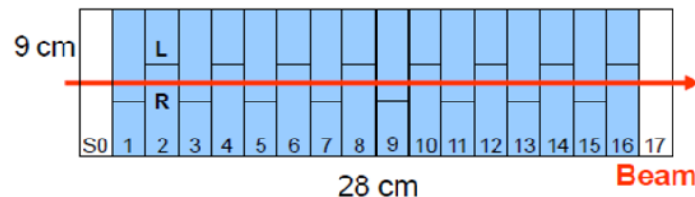


MUSIC detector

MUlti-Sampling Ionization Chamber



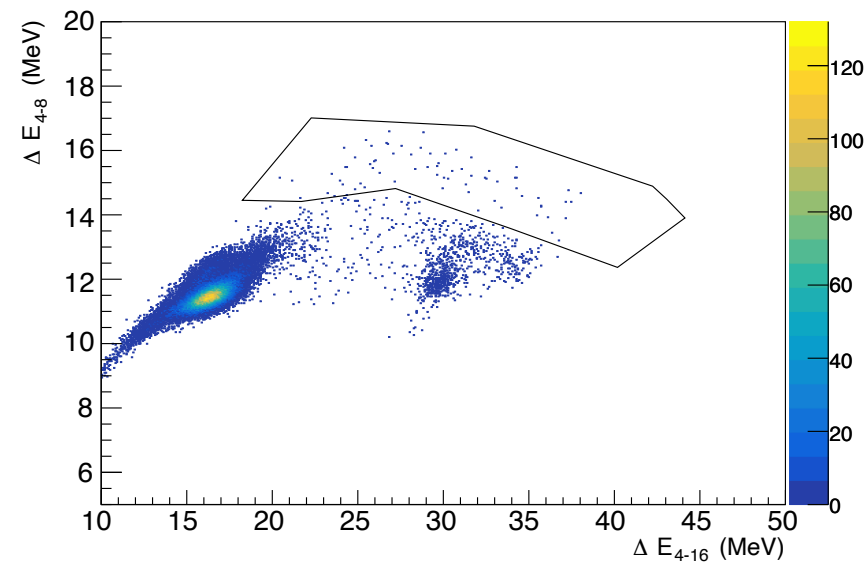
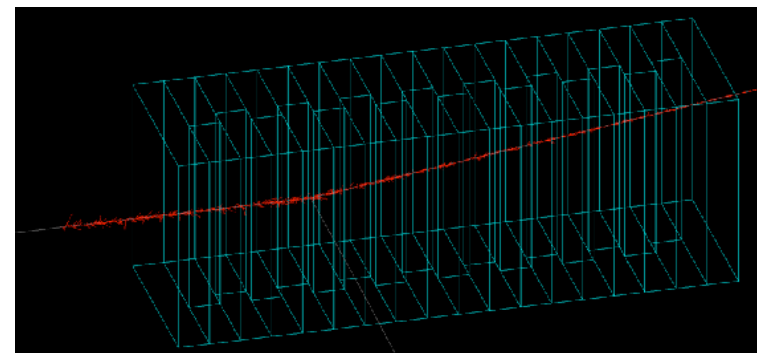
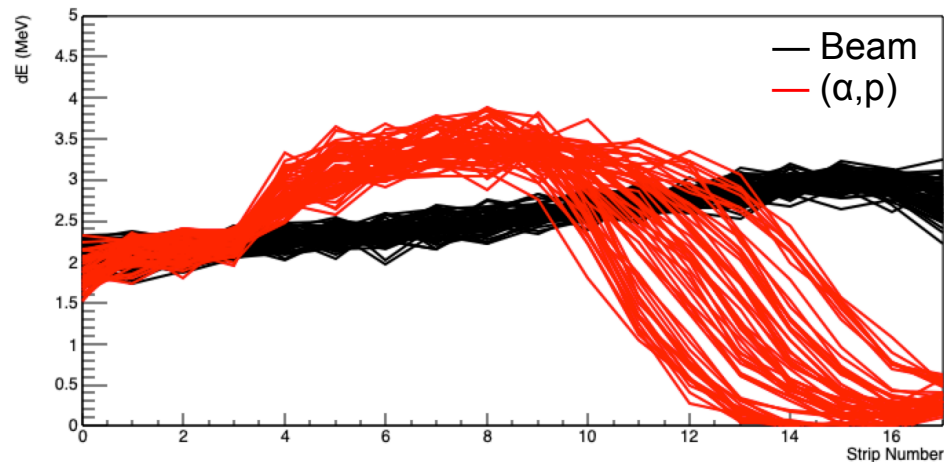
Schematic of the anode structure



- Active target detector
- MUSIC offers a high efficiency due to the segmented anode structure.
This allows to measure a wide energy range with just a single beam energy.
- MUSIC is self-normalizing.
Absolute normalization can be obtained with no additional monitor detectors.
- Gases: ^4He , $^{20,22}\text{Ne}$, Ar, CH_4 , etc
- Pressures: 150 - 760 Torr

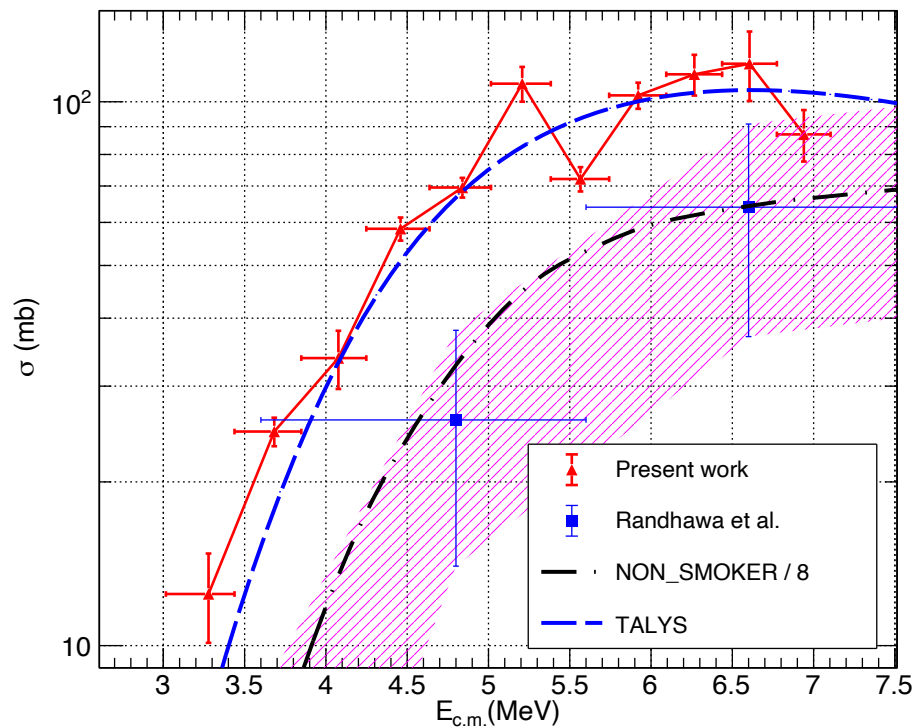
Particle identification

Events occurring in Strip 4 of MUSIC



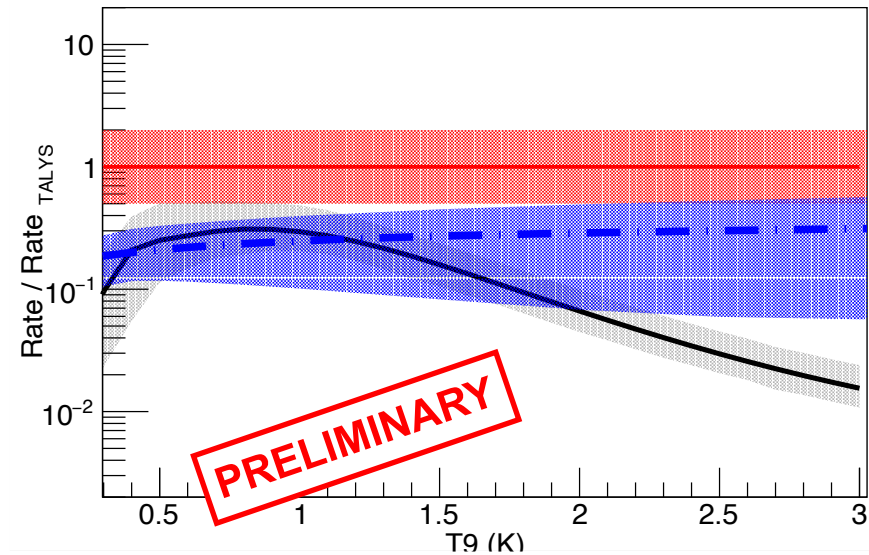
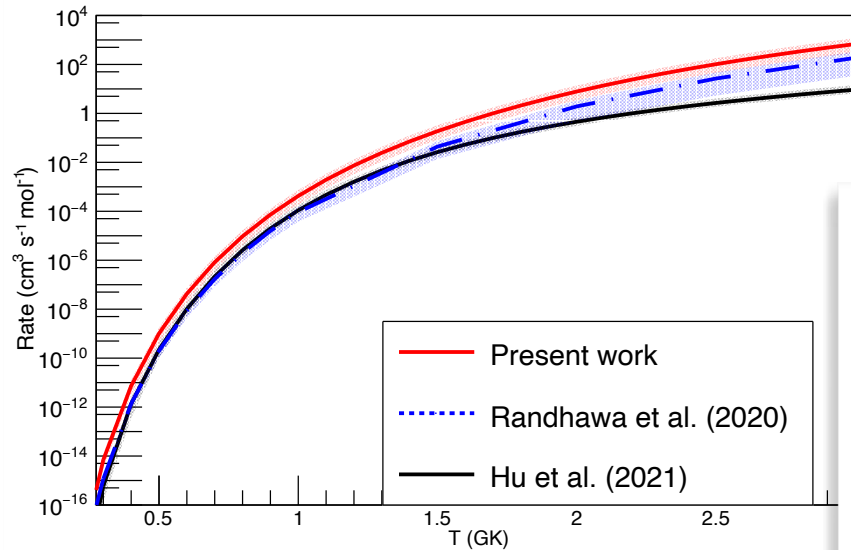
Total reaction cross section

$^{22}\text{Mg}(\alpha, p)$ Cross Section



- TALYS calculations performed by P. Mohr using McFadden & Satchler α -OMPs .
- Experimental CS are in good agreement with theoretical TALYS CSs within a factor of 2.
- Total reaction cross sections from the present work are higher than those of Randhawa et al. (2020)

Reaction rate comparison



SUMMARY

- A direct measurement of the $^{22}\text{Mg}(\alpha, p)^{25}\text{Al}$ reaction was performed using MUSIC at ATLAS.
- Total reaction cross sections are presented.
- Total reaction cross section is in good agreement with TALYS predictions within a factor of 2.
- Astrophysical implications are currently under investigation.



M. Avila

D. Santiago-Gonzalez

C. R. Hoffman

K. E. Rehm

T. L. Tang

C. Muller-Gatermann

B. P. Kay

M. Carpenter

K. Teh

D. Potterveld

J. Chen



G. Wilson



Tan Ahn



Z. Meisel



C. Ugalde

D. Neto



W. J. Ong



T. Psaltis



Johnson Liang



THANK YOU



Argonne National Laboratory is a
U.S. Department of Energy laboratory
managed by UC Chicago Argonne, LLC.

